Applied Acoustics 186 (2022) 108461

Contents lists available at ScienceDirect

Applied Acoustics

journal homepage: www.elsevier.com/locate/apacoust

An ultrasonic signal reconstruction algorithm of multilayer composites in non-destructive testing

Yiming Li, Kai Yao *, Xinglong Li

Department of Mechanics, School of Civil Engineering, Beijing Jiaotong University, Beijing 100044, China

ARTICLE INFO

Article history:
Received 23 March 2021
Received in revised form 30 September 2021
Accepted 7 October 2021
Available online 29 October 2021

Keywords:
Non-destructive testing
Ultrasound
Signal processing
MP algorithm
Multilayer structure

ABSTRACT

With the wide application of composite materials in various fields, efficient and reliable non-destructive testing technology has been developed in a general manner. Due to the technical constraints and environmental changes in the composite material preparation process, there are many defects, such as debonding and unequal thickness. Ultrasonic testing, being a non-destructive testing method, has been widely used in many areas because of its convenience and effectiveness. In this paper, a new self-interference cancellation algorithm based on the matching pursuit algorithm is proposed, which can eliminate the waveform generated by multiple reflections in the echoed signal. A two-dimensional finite element model with multiple defects of composite materials is established to simulate the actual process of damage detection. The calculated damage location is compared with the model's actual parameters, which shows that the algorithm can be applied to the defect location of multilayer composites. A multilayer structure ultrasonic experiment is established and the good performance of the algorithm has been verified.

1. Introduction

In recent years, composite materials, because of their high specific strength and corrosion resistance, have been widely applied in many areas, such as the manufacturing industry, aerospace industry, construction industry. However, various defects inevitably occur in the preparation and service of composite materials, including microcracking, voids, delamination, and debonding [1,2]. These problems may lead to the strength and service life of the material dropping off more sharply than expected. Therefore, non-destructive testing (NDT) methods have gradually received widespread attention to ensure the safety and reliability of composite materials. Unlike homogeneous materials, composite materials have a new microstructure, the "interface", which is between two different layers, where most of the defects lie. Thus, accurately and quickly locating the position and estimating the size of the "interface" is an excellent way to evaluate the defect in the process of testing. Common NDT methods for composite materials include ultrasonic testing (UT), visual testing (VT), radiographic testing (RT), and electromagnetic testing (ET) [3].

Ultrasound detection has been received with great expectations because it has the advantages of simple equipment, simple operation, a large detection area, and high sensitivity to defects. The existing ultrasonic pulse-echo (PE) method has been widely used to detect defects for such determination[4,5]. Elena et al. used the immersion pulse-echo technique with a novel signal post-processing algorithm for the non-destructive evaluation of composite adhesive joints [6]. Nie et al. proposed a parameter estimation method of ultrasonic echo combining minimum entropy deconvolution with the expectation–maximization (EM) algorithm [7]. Mastan et al. used array transducer analysis to interpret the impact damage results of carbon fiber sandwich materials. Compared with the unit sensor, the array sensor has good defect detection ability. It is the most straightforward process to detect impact damage in less time [8]. The most important thing is to accurately determine the damage signals' position in the waveforms. The matching pursuit (MP) algorithm is based on sparse decomposition, which is proposed to match the fault signals [9]. Ruiz-Reyes et al. presented a novel high-resolution pursuit (HRP is a version of MP) based method to detect flaws close to the material surface in ultrasonic NDT of highly scattering materials. Based on the use of a new correlation function, the method allows for emphasizing local fit over global fit at each iteration and can efficiently eliminate grain noise and increase the visibility of ultrasonic flaw signals [10]. Kim et al. proposed a way of detecting damage with a limited number of transducers on a plate using a Hann-windowed tone-burst excitation atom dictionary that can be

* Corresponding author.
E-mail address: kaiy@bjtu.edu.cn (K. Yao).

https://doi.org/10.1016/j.apacoust.2021.108461
0003-682X/

applied to locate the damage determination in a composite plate [11]. Li et al. developed a correlation filtering-based matching pursuit (CF-MP) signal processing approach. It aims to identify both the location and the size of delamination in the composite beams [12]. Tse et al. reported a new method of MP equipped with an optimized dictionary by analysing the interference between the reflection components embedded in a defect reflection signal to enable efficient extraction of defect information. The method can effectively resolve the closely spaced overlapping and noise-contaminated reflection components [13]. To a certain extent, the pulse-echo method can obtain information on the location, depth, and size of the defects. Zhang et al. used laser ultrasonic technique to detect disbonds in a multi-layer bonded structure base on pulse-echo mode. The experimental results show pulse-echo mode detection of disbonds in multi-layer bonded structures was practicable [14]. However, this method has some disadvantages with high interference due to the multiple reflections of multilayer materials. In detecting the depth of defects, it is necessary to eliminate multiple echoes and accurately analyse the damage interface signals' position in waveforms. Zheng et al. used a wavelet transform signal analysis method based on the high-power ultrasonic scan to detect the debonding defects in the composite. The result shows their method could reduce the interference of layer overlap to a certain extent [15]. The purpose of this study is to develop a new signal processing method of ultrasonic pulse-echo signal processing based on the MP algorithm, which uses the layer-by-layer iteration procedure to self-interference cancellation. This approach can determine the location and size of multiple damages.

2. Signal processings

The signal waveform usually becomes overly complicated when it is superimposed with noise, boundary reflections, and other factors. It is challenging to find the corresponding damage waveform directly from the ultrasonic A-scan waveform. Thus, to accurately locate the damage waveform based on the damage waveform characteristics, we need to process the signal reasonably.

2.1. MP algorithm

The MP method is a classical sparse decomposition method and one of the conventional adaptive signal processing methods. The MP method can decompose the complex pre-analysis signal and denoise it by constructing a vast redundant waveform dictionary. Through repeated iterative steps, the signal is projected onto the dictionary, and the waveforms matching the pre-analysis signal are selected. Then, the signal is decomposed on the dictionary after passing through the continuous iterative operation. This method can be expressed as finding a group of bases in the dictionary to represent the signal. The process of expressing a signal with a specific group of bases actually finds the corresponding expansion coefficients. The procedure is as follows.

(1) y is used the label for the ultrasonic testing signal with length n and the waveform dictionary$D = \{d_i\} \in R^{n\times m}$ is established.
(2) The iteration counter $k = 1$ and the signal residual $r^{(0)} = y$ are initialized.
(3) The dictionary is searched for the best correlate atom d_k, which has the maximum inner product value with the residual $r^{(k-1)}$:

$$d_k = argmax_{d_k \in D} \left| \langle r^{(k-1)}, d \rangle \right|. \tag{1}$$

(4) The signal residual r^k can be obtained by subtracting its projection on d_k from the residual $r^{(k-1)}$:

$$r^k = r^{(k-1)} - \langle r^{(k-1)}, d_k \rangle d_k. \tag{2}$$

(5) The steps (3) and (4) are iterated with $k = k + 1$ until the signal residual meets the requirement.

Finally, we can decompose the signal y into:

$$y = \sum_{i=1}^{K} \langle r^{(i-1)}, d_i \rangle d_i + r^{(K)}, \tag{3}$$

where$K$ is the number of cycles necessary to meet the requirement.

2.2. Dictionary design

In the MP method, because the waveform dictionary is not constrained, the MP method has strong adaptability and flexibility in signal decomposition and reconstruction. Traditional waveform dictionaries are usually constructed with Gabor or chirped atoms [16,17]. By adjusting the frequency, pulse width, amplitude, phase, and other parameters, the atom in the waveform dictionary is established. In obtaining higher resolution and improving the processing speed to find the signal's sparsest representation, it is necessary to build an optimized waveform dictionary by associating the known signal waveform and incorporating the signal reflection characteristics. In this paper, the atoms in the waveform dictionary are constructed by adjusting the frequency, time shift, scale, and phase based on the input signal which can be expressed as:

$$g(t) = As(2\pi f_c(t - T) + \theta), \tag{4}$$

where $s(t)$ is the input signal waveform, A is the scale factor, f_c is the frequency factor, T is the time shift factor, θ is the phase factor.

3. Damage detection

3.1. PE method

When the ultrasonic signal p_i encounters the interface between two layers with dissimilar acoustic impedances, it produces a transmission signal p_t and reflection signal p_r at the interface, as shown in Fig. 1. There are multiple paths of the reflection signals from different interfaces in the specimen. The PE method, a widely used NDT method, tries to find the corresponding damage waveforms from the A-scan signal. Then, one can use the waveform flight time to locate the defect depth according to the equation:

$$d = \frac{v(t_1 - t_2)}{2}, \tag{5}$$

where v is the velocity of sound in the material, t_1 is the flight time of the specimen surface and t_2 is the flight time of the defect.

3.2. Elimination of multiple echoes

In the ultrasonic PE method of multilayer materials, multiple echo peaks overlapping in the acquisition signal were investigated in three kinds of wave paths: (1) arriving directly by reflection from only one interface, (2) reflected many times from multiple interfaces, and (3) reflected from the boundaries of a plate. In this paper, the infinite plate case is considered, so the influence of (3) is ignored. The first case is the primary reflection wave, and the second case is regarded as interference waves. Fig. 2, I, II, III, and IV show four main echo paths composed of the reflection

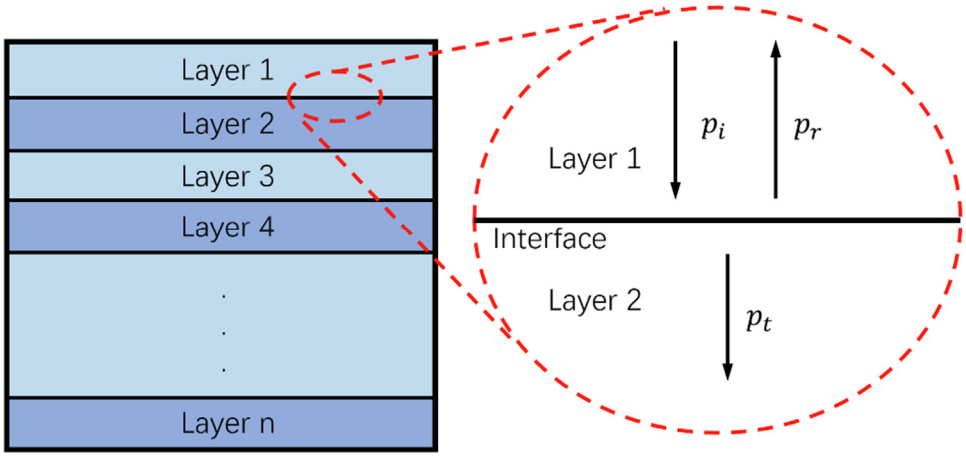

Fig. 1. Reflection and transmission at the interface of the multilayer structure.

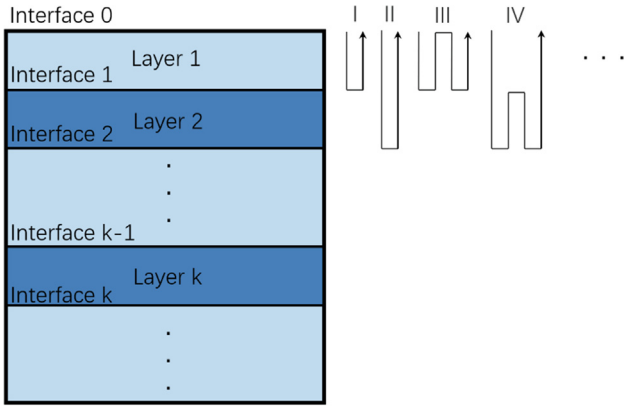

Fig. 2. Wave paths of the echoes.

and transmission of the acoustic wave at the interfaces. I and II belong to case (1), while III and IV belong to case (2). Although all echo paths reflect the information of the interfaces inside the specimen to varying degrees, paths I and II can be used more efficiently. However, there are many overlaps between the primary reflection waves, and the interference waves make the interface location difficult. In this paper, the waveform formed by multiple reflections can be effectively reduced by the iterative self-cancellation method. The principle is:

(1) The waveforms transmitted by the probe are indicated on interface 1 and reach interface 0. The probe receives the transmitted wave as a reflected wave, which is incident from interface 0 to the specimen's interior again and brings an interference signal. In the vertical direction where the probe is located, this interference signal waveform is the same as the probe's directly excited, except for time shift and amplitude. If the waveform transmitted by the probe and the waveform finally received are recorded as $p(t)$ and $y(t)$, then the waveform reflected by interface 1 and interface 0 can be expressed as $Ap(t-T)$, where A is the amplitude loss, which is composed of reflection coefficients of interface 1 and interface 0 and the energy loss during signal propagation, T is time shift determined by the flight time when the signal reaches interface 1 and returns. Because the propagation distance is the shortest, the first wave packet in the received signal $y(t)$ can be identified as the reflection waveform of interface 1 with the flight time T_1. The waveform probe received of the interference signal caused by interface 1 can be expressed as:

$$u_M^{(1)} = Ay(t - T_1), \tag{6}$$

where A is the amplitude loss and $y(t)$ is the signal collected from the ultrasonic probe.

(2) To analyse the reflection wave packet from interface 2, the reflection signal $u_{R1}(t)$ and the interference signal $u_M^{(1)}$ are deducted from the acquisition signal $y(t)$. The first wave packet in the residual signal can be determined as the reflection wave of interface 2 (because it has the shortest transmission distance).

(3) By iterating steps (1) and (2), the original signal can be effectively denoised, and the direct reflection wave packet and their flight time from each interface can be obtained. At the same time, the waveform containing only the primary wave can also be obtained.

The original signal itself often carries many other interference signals (external environment interference, etc.). For PE mode ultrasonic inspection, the A-scan signal u_t of the multilayer structure can be written as the superposition of the echoes reflected from different interfaces [18]:

$$u_t(t) = \sum_{i=1}^{M} s_i(t) + \xi(t), \tag{7}$$

where M is the number of reflected echoes, $s_i(t)$ is the waveform corresponding to each interval, and $\xi(t)$ is the structural noise. The self-interference cancellation algorithm mainly aims at eliminating the influence of multiple reflection waveform, that is, filtering out the interference in $\sum_{i=1}^{M} s_i(t)$. Therefore, an initial signal without external noise is easier to get accurate results, meaning $\xi(t)$ need to be reduced as possible. The procedure is:

(1) The MP algorithm (introduced in chapter 2) is used to reduce the influence of external noise. By adjusting the frequency, time shift and scale of the input signal, the waveform dictionary of MP algorithm can be generated. The ultrasonic signal $u_t(t)$ acquired from receiving transducer is decomposed and reconstructed by MP algorithm and get the signal $u_M(t)$ which has been eliminate the external environment interference.

(2) The residual signal is initialized:

$$y^{(0)}(t) = \begin{cases} u_M(t), t \geq 0 \\ 0, t < 0 \end{cases}. \tag{8}$$

(3) The waveform with the shortest flight time can be obtained from the residual signal $y^{(N-1)}(t)$ slated as the reflection waveform at the number N interface (the primary reflection wave), where the signal waveform is denoted as $u_{RN}(t)$, while the flight time is denoted as T_N (define $T_0 = 0$).

(4) The waveforms corresponding to the multiple reflection signals between interface N and the last $N - 1$ interfaces are calculated:

$$u_M^{(N)} = \sum_{k=1}^{N} r_{N,k} \alpha y^{(k-1)}(t - (T_N - T_{k-1})), \tag{9}$$

where α is the energy reduction factor in the process of wave propagation in the medium and $r_{N,k}$ is the reflection coefficient that can be taken from matrix r:

$$r = \begin{bmatrix} R_1R_0 & 0 & 0 & & 0 \\ (1-R_1)^2R_2R_0 & (1-R_1)^2R_2R_1 & 0 & \cdots & 0 \\ (1-R_1)^2(1-R_2)^2R_3R_0 & (1-R_1)^2(1-R_2)^2R_3R_1 & (1-R_1)^2(1-R_2)^2R_3R_2 & & 0 \\ & \vdots & & \ddots & \vdots \\ (1-R_1)^2(1-R_2)^2\cdots R_NR_0 & (1-R_1)^2(1-R_2)^2\cdots R_NR_1 & (1-R_1)^2(1-R_2)^2\cdots R_NR_2 & \cdots & (1-R_1)^2(1-R_2)^2\cdots R_NR_{N-1} \end{bmatrix} \tag{10}$$

where R_i is the reflection coefficient of interface number i. This coefficient can be calculated from the echo amplitude or according to the equation:

$$R_i = \frac{Z_{i+1} - Z_i}{Z_{i+1} + Z_i} \tag{11}$$

where $Z = \rho \cdot c$ (ρ and c are the density and wave velocity, respectively) is the acoustic impedance.Z_{k-1} is the acoustic impedance of the first propagating medium, while Z_k is that of the second propagating medium.Z_0 is the acoustic impedance of the specimen surface.

(5) The residual signal $y^{(N)}(t)$ can be obtained according to the equation:

$$y^{(N)}(t) = y^{(N-1)}(t) - u_{RN}(t) - \sum_{k=1}^{N} r_{N,k} y^{(k-1)}(t - (T_N - T_{k-1})) \tag{12}$$

(6) The steps (3), (4), and (5) are iterated with $N = N + 1$ until the residual signal meets the requirement.

Finally, after eliminating the multiple echoes, we can acquire the main-wave signal $u_F(t)$:

$$u_F(t) = \sum_{i=1}^{N} u_{RN}(t). \tag{13}$$

4. Finite element analysis

To accurately analyse the location of the defects in composite materials, a two-dimensional (2D) plane strain finite element (FE) model is developed using COMSOL Multiphysics for the simulation of ultrasonic wave propagation.

4.1. FEM model establishment

The composite is modelled for longitudinal wave propagation, and a simple rectangular geometry is chosen with dimensions of 240 mm × 80 mm. Simultaneously, two perfectly matched layers (PMLs) are set at the left and right sides of the model to avoid reflection, as shown in Fig. 3. The thickness of the carbon fiber layers is 60 mm, with each thickness of two copper layers being 10 mm. In addition, a defect layer with a thickness of 15 mm and depth (distance to the top) of 25 mm has a Young's modulus loss of 30% compared to the non-defective area. The material parameters of the composite sample are shown in Table 1.

Quadrilateral elements are used for grid division. The size of each unit is chosen by the criteria $\lambda_L/\Delta x = 8$, where λ_L is the minimum wavelength within the bandwidth of the signal. The minimum mesh quality for each model solved is 0.7, with an element area ratio of approximately 0.1. The time steps used are $1/(100 \times f_c)$, where f_c is the frequency of the signal [19–21].

The ultrasonic probe is arranged on the top side of the model plate. It is a dual-crystal probe with a size of 10 mm ×0.2 mm used to activate and receive the signal.

A 2.5 MHz frequency signal is applied to the PZT. The signal is chosen as five cycles of the cosine function and tuned by the Hann window:

$$V(t) = 0.5\left(1 - \cos\frac{2\pi f_c t}{n_p}\right)\sin(2\pi f_c t), \tag{14}$$

where f_c is the central frequency and n_p is the period number. In this study, $f_c$and n_p are chosen as 2.5 MHz and 5, respectively.

The time-domain representation of the input pulse is shown in Fig. 4. The frequency content of the input signal was evaluated as the Fourier transform of the time domain signal, as shown in Fig. 5.

4.2. Signal analysis

The resulting voltage output is plotted in Fig. 6 for 30 μs, where artificial Gaussian white noise (GWN) is added to the measured signal, of which the signal-to-noise ratio (SNR) is approximately 6.5 dB. By reconstructing the original signal with the MP algorithm, several wave packet locations can be found, numbered I, II, III, IV and V. The comparison results of these two signals show that the MP algorithm has a significant effect in eliminating environmental noise. Some waveforms hidden in the interference signal can also

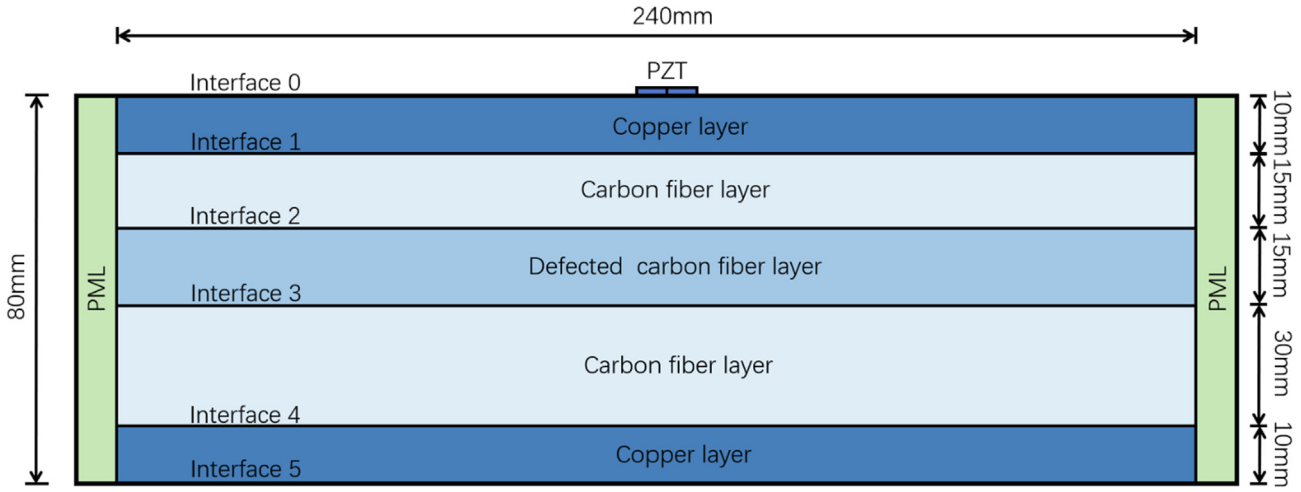

Fig. 3. 2D Finite Element Model.

Table 1
Material parameters of the sample.

Properties	Symbol	Carbon fiber	Copper	Unit
Young's modulus	E	5.48E10	1.28E11	Pa
Poisson's ratio	υ	0.33	0.30	–
Density	ρ	1710	8930	kg/m^3

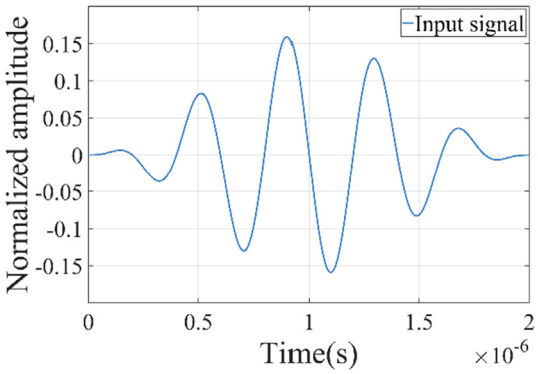

Fig. 4. Input signal waveform.

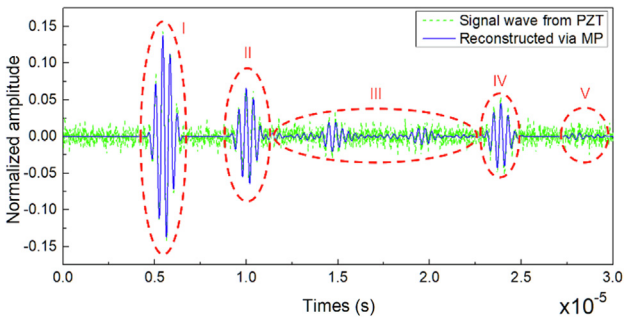

Fig. 6. Original signal and signals reconstructed via MP.

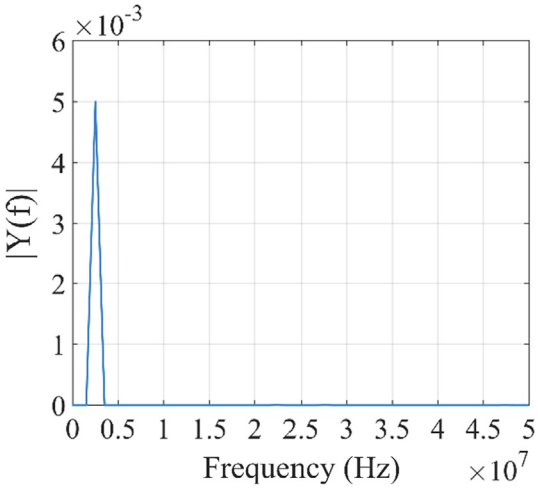

Fig. 5. Input signal in the frequency domain.

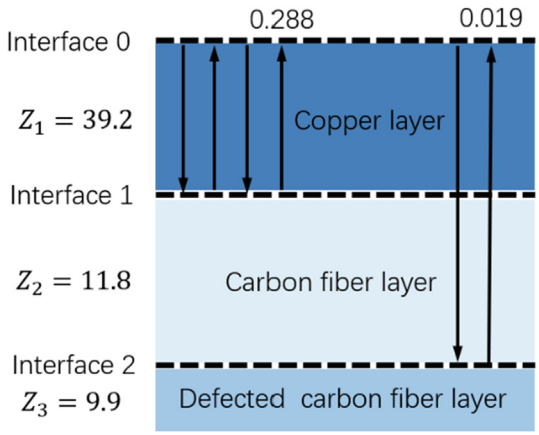

Fig. 7. Calculated normalized amplitude values of the received signal for two different wave paths.

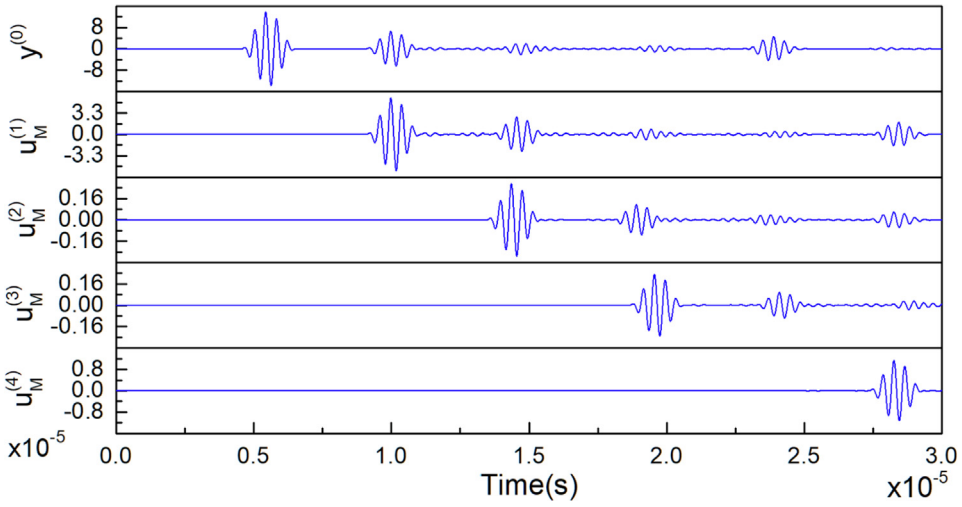

Fig. 8. Initial signal residual $y^{(0)}$ and waveforms corresponding to the multiple reflection signals.

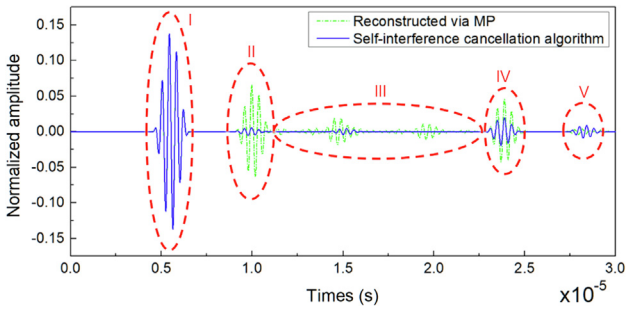

Fig. 9. Signal reconstructed via MP and signal processed by the self-interference cancellation algorithm.

be displayed, such as region III. However, by analysing the reconstructed signal via the MP algorithm, it is shown that this method is invalid for the decomposition of multiple overlapping signals. Wave packets in regions I, II and IV are relatively independent and integrated.

In contrast, the waveforms in regions III and V are not clearly separated from each other due to the interference caused by multiple reflections, making it challenging to obtain the wave packet TOFs accurately. In addition, as shown in Fig. 7, because the acoustic impedance of the media on both sides of interface 1 are quite different, the reflected signal amplitude is much larger than that reflected from interface 2. Normalized amplitude values of the second-reflected signal between interface 0 and interface 1 are ten times more than the single-reflection signal from interface 2, which brings significant interference to the signal analysis process.

Fig. 8 shows the initial signal residual $y^{(0)}$ and waveforms corresponding to the multiple reflection signals u_m. u_m^4 indicates the overlapping signal of multiple reflected waveforms formed between interface 4 and the previous four interfaces. The same goes for u_m^1, u_m^2 and u_m^3. Fig. 9 shows a comparison between the signal reconstructed by the MP algorithm and the self-interference cancellation algorithm. Table 2 shows the TOFs and their errors of each interface reflected signal analysed by these two algorithms. The theoretical value is calculated by formula 14. The error of the results obtained by the self-interference cancellation algorithm is significantly reduced compared with that of the MP analysis results. Simultaneously, for interfaces 3 and 5, the MP algorithm cannot determine the interface position due to interference, and the self-interference cancellation algorithm can find the interface position with minimal error.

$$t_n = 2 \times \left(\frac{d_1}{v_1} + \frac{d_2}{v_2} + \cdots + \frac{d_n}{v_n} \right) \tag{15}$$

where d_n is the thickness of medium n and v_n is the velocity of sound in medium n.

The waveform of region I in Fig. 9 represents the reflected wave of interface 1, and its TOF is 4.55 μs. Since the TOF of the signal reflected from interface 1 is the shortest, there are no multiple overlapping signals. The reconstructed waveforms of the two algorithms are consistent. The blue line in region II represents the reflection wave from interface 2, and its TOF is 8.93 μs, with a relative error of 0.26% compared with the theoretical value. The green line is the superposition of the interface 2 reflection wave and multiple reflection waveforms. The multiple reflection signals are mainly composed of a double-reflection waveform between interface 0 and interface 1, and its TOF is 9.10 μs. The wave packet formed by interface 2 has a TOF similar to that of the double-reflection waveform. Nevertheless, the amplitude is much smaller, which means that it cannot be found accurately without a self-interference cancellation algorithm, resulting in an error of 2.17%. The situation of regions III and IV is similar to that of region II: due to the interference of multiple reflection waves, the original interface reflection waves are suppressed, and signal analysis cannot be carried out accurately. In addition, owing to the continuous waveform and multiple wave packets with large amplitudes at position III, the reflected signal of interface 3 cannot be determined. After self-interference cancellation processing, the TOF of

Table 2
TOF of reflected waves at each interface (errors).

Methods	Interface 1	Interface 2	Interface 3	Interface 4	Interface 5
Theory	4.553	8.907	14.11	22.818	27.371
MP	4.55 (0.06%)	9.10(2.17%)	Unknown	22.87(0.23%)	Unknown
self-interference cancellation	4.55 (0.06%)	8.93(0.26%)	14.15(0.28%)	22.84(0.10%)	27.40(0.11%)

TOF is the time of flight, units: μsec.

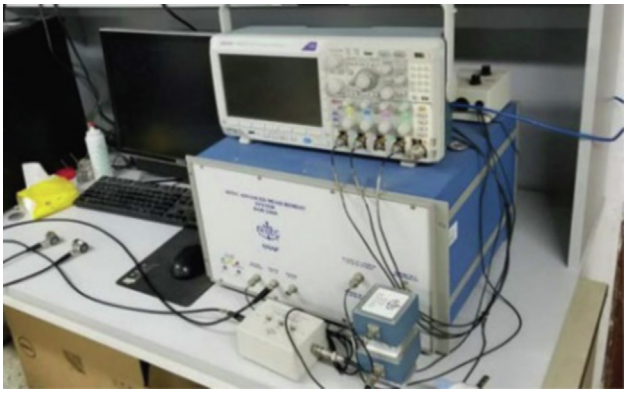

Fig. 10. Ultrasonic testing equipment.

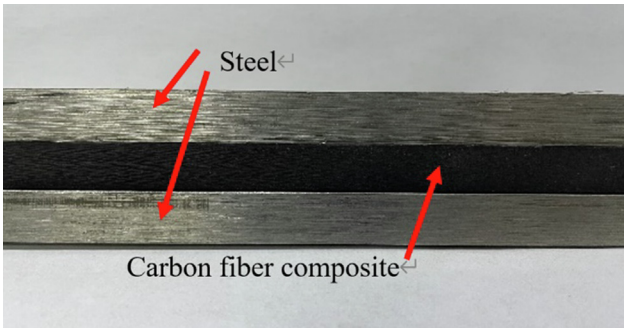

Fig. 11. Experimental sample.

the interface can be found accurately, with an error of 0.28%. Region 5 is different. The difference between the two lines shows that due to the influence of multiple reflected waves, the amplitude formed by interface 5 is significantly weakened, making it suppressed in the interference. The main reason is that the TOFs of the two paths (transducer-interface 1-interface 0-interface 4-transducer; transducer-interface 4-interface 0-interface 1-transducer) are equal to the single-reflection signal of interface 5. There is a half-wave loss in these two paths, which weakens the signal amplitude.

5. Experimental results

In this study, to test the performance of the proposed signal processing technique, experiments were carried out on the multi-layer structure of steel with carbon fiber composites, as shown in Fig. 11. The width and the length are given by 200 mm × 200 mm. The thickness of the two steel plates is 10 mm, while the CFRP layer thickness is 9 mm. The adhesive used to bond the CFRP with the steel is epoxy resin. The ultrasonic testing system SNAP-5000 (Ritec, USA) was used to generate a tone burst type signal with a 2.5 MHZ frequency, which is shown in Fig. 10. A double crystal probe was used to excite and receive the reflected signal, and the reflected signal is measured five times and averaged to ensure a better signal-to-noise ratio.

A finite element model with the same size as the test is established to ensure the accuracy of the results. The resulting voltage output is plotted in Fig. 13 for 14 μs. By comparing the signal waveform with the signals reconstructed via MP in experimental, MP processing can effectively reduce external noise interference.

Fig. 12 shows the ultrasonic signal collected by the transducer and signals reconstructed via MP and self-interference cancellation algorithm. In the signal waveform shown in Fig. 12(a), due to the interference of the noise signal, it is difficult to find other ordered waveforms except for three evident wave packets, which are numbered I, II, and III, and much less so to locate the position of the wave packet. If the position cannot be determined, the damage or the medium's interface cannot be judged, bringing great difficulties to non-destructive testing. However, after signal processing, as shown in Fig. 12(b), we can still find the three most apparent wave packets numbered IV, V, and VI, but the flight time of the V wave packet is different from that of wave packet II in Fig. 12(a). Simultaneously, the position of wave packet II in Fig. 12(b) displays nothing but noise. The self-interference cancellation algorithm eliminates the interference waveform caused by the multiple reflections from the interface M on the signal. The original reflection waveform of interface N can be found. At this time, the

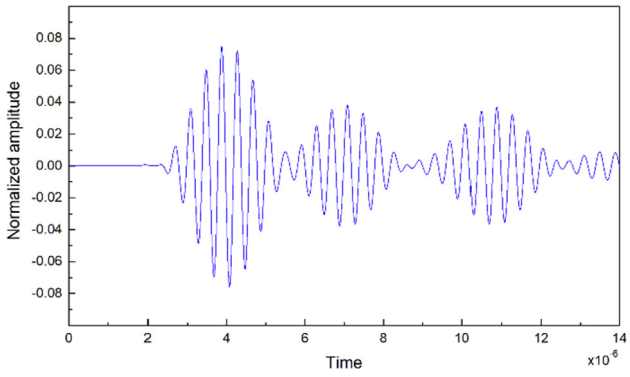

Fig. 13. Original signal received by the probe in numerical simulation(a).

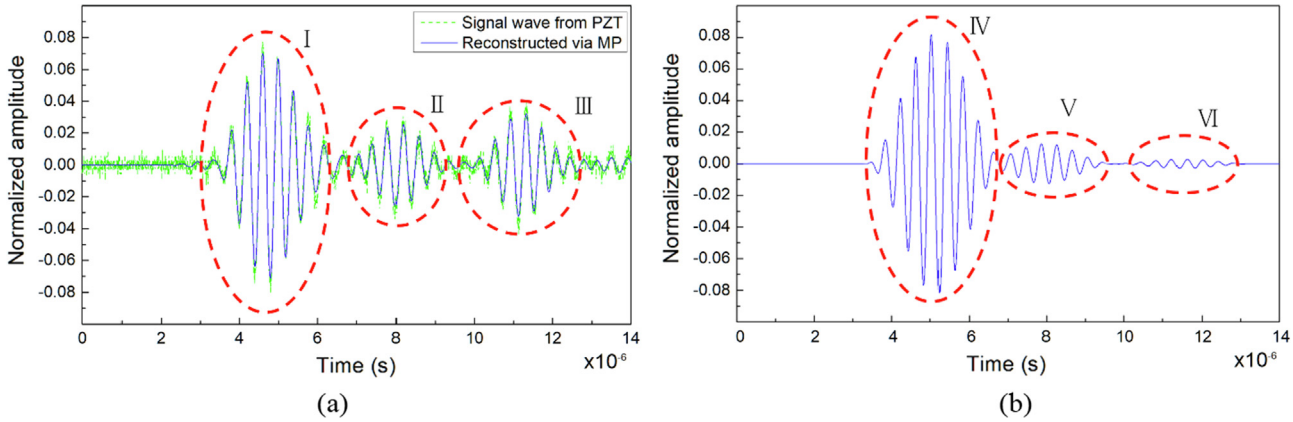

Fig. 12. Original signal and signals reconstructed via MP (a) and signals processed by the self-interference cancellation algorithm (b).

Table 3
Comparison of the predicted depth and the degree of damage.

Interface	Calculated depth in experimental	Error	Real depth	Calculated depth in numerical simulation	Error
Interface M	10.07	0.70%	10	10.008	0.008%
Interface N	19.22	1.16%	19	18.979	0.111%
Interface P	29.35	1.21%	29	28.941	0.203%

position of the material interface or defective interface can be calculated by the corresponding ultrasonic flight time of three-wave packets, which is shown in Table 3. As a comparison, the interface position calculated by the signal collected through numerical simulation is also given in Table 3. Because the environment of numerical simulation is more ideal than that of experiment, the results is more accuracy.

6. Conclusion

A two-step signal processing algorithm for an ultrasonic pulse-echo waveform that includes multiple wave paths of damage detection was presented. The received signals first eliminated noise using the matching pursuit (MP) algorithm, an adaptive signal processing technique. In this study, the atom of the MP dictionary is formed with Hann-windowed tone burst excitation. Signals were then analysed using a layer-by-layer iteration procedure for self-interference cancellation. This procedure's objective function is reducing or even eliminating the proportion of multiple reflected wave energies in the received signals, which can strongly affect the procedure for locating multilayer damage. The performance of the proposed algorithm was investigated considering laminated composites with multiple types of damage. The studies presented in this paper indicate that the proposed approach is an efficient way to reduce the noise and find the main path wave packet (single-reflection wave path). The simulation and experimental results show that this algorithm can effectively and accurately separate multiple overlapping signals and eliminate interference compared with the traditional method. It can make the interface position that can be found more accurate and reconstruct the wave packet submerged by interference, thus significantly improving the readability of multilayer composite ultrasonic signal detection.

Moreover, this method can find the reflected signal submerged in noise and restore the waveform lost due to signal superposition and cancellation. This research will improve the speed and accuracy of the ultrasonic pulse-echo method for damage location of multilayer structures. Furthermore, this algorithm can automatically eliminate noise interference and locate the main path wave packet. Combining with a neural network will be very convenient to achieve the precise damage location of composite materials.

CRediT authorship contribution statement

Yiming Li: Conceptualization, Methodology, Software, Validation, Writing - original draft. **Kai Yao:** Conceptualization, Methodology, Writing - review & editing, Funding acquisition, Supervision. **Xinglong Li:** Software, Data curation, Validation.

Declaration of Competing Interest

The authors declare that they have no known competing financial interests or personal relationships that could have appeared to influence the work reported in this paper.

Acknowledgments

Project supported by the National Natural Science Foundation of China (No. 11872104) and Fundamental Research Funds for the Central Universities (2019JBM82).

References

[1] Sihn S, Kim R, Kawabe K, Tsai S. Experimental studies of thin-ply laminated composites. Compos Sci Technol 2007;67(6):996–1008. https://doi.org/10.1016/j.compscitech.2006.06.008.
[2] Bastianini F, Di Tommaso A, Pascale G. Ultrasonic non-destructive assessment of bonding defects in composite structural strengthenings. Compos Struct 2001;53(4):463–7. https://doi.org/10.1016/S0263-8223(01)00058-7.
[3] Gholizadeh S. A review of non-destructive testing methods of composite materials. Procedia Struct Integrity 2016;1:50–7. https://doi.org/10.1016/j.prostr.2016.02.008.
[4] Benammar A, Drai R, Guessoum A. Detection of delamination defects in CFRP materials using ultrasonic signal processing. Ultrasonics 2008;48(8):731–8. https://doi.org/10.1016/j.ultras.2008.04.005.
[5] Guyott CCH, Cawley P, Adams RD. The Non-destructive Testing of Adhesively Bonded Structure: A Review. Journal of Adhesion - J ADHES. 1986;20(2):129–59. https://doi.org/10.1080/00218468608074943.
[6] Jasiūnienė E, Mažeika L, Samaitis V, Cicėnas V, Mattsson D. Ultrasonic non-destructive testing of complex titanium/carbon fibre composite joints. Ultrasonics 2019;95:13–21. https://doi.org/10.1016/j.ultras.2019.02.009.
[7] Nie X, Guo Z, He Z, Cheng A, Ji Y. Parameters estimation of ultrasonic echo signal based on blind deconvolution and parameterized model. Chinese journal of scientific instrument 2015;36:2611–6.
[8] Papanaboina M, Manimaran H, Kommanaboyina NM, Jasiuniene E. Analysis of defects in the carbon fiber sandwich material using ultrasonic methods. Conference of Young Scientists Industrial Engineering 2018;2018.
[9] Mallat SG, Zhang Z. Matching pursuits with time-frequency dictionaries. IEEE Trans Signal Process 1993;41(12):3397–415. https://doi.org/10.1109/78.258082.
[10] Ruiz-Reyes N, Vera-Candeas P, Curpián-Alonso J, Cuevas-Martínez JC, Blanco-Claraco JL. High-resolution pursuit for detecting flaw echoes close to the material surface in ultrasonic NDT. NDT and E Int 2006;39(6):487–92. https://doi.org/10.1016/j.ndteint.2006.02.002.
[11] Kim HW, Yuan FG. Enhanced damage imaging of a metallic plate using matching pursuit algorithm with multiple wavepaths. Ultrasonics 2018;89:84–101. https://doi.org/10.1016/j.ultras.2018.01.014.
[12] Li F, Su Z, Ye L, Meng G. A correlation filtering-based matching pursuit (CF-MP) for damage identification using Lamb waves. Smart Mater. Struct. 2006;15(6):1585–94. https://doi.org/10.1088/0964-1726/15/6/010.
[13] Tse PW, Wang XJ. Characterization of pipeline defect in guided-waves based inspection through matching pursuit with the optimized dictionary. NDT and E Int 2013;54:171–82. https://doi.org/10.1016/j.ndteint.2012.10.003.
[14] Zhang K, Li S, Zhou Z. Detection of disbonds in multi-layer bonded structures using the laser ultrasonic pulse-echo mode. Ultrasonics 2019;94:411–8. https://doi.org/10.1016/j.ultras.2018.06.005.
[15] Zheng S, Zhang S, Luo Y, Xu B, Hao W. Nondestructive analysis of debonding in composite/rubber/rubber structure using ultrasonic pulse-echo method. Nondestructive Testing and Evaluation 2021;36(5):515–27. https://doi.org/10.1080/10589759.2020.1825707.
[16] Cui L, Wang J, Lee S. Matching pursuit of an adaptive impulse dictionary for bearing fault diagnosis. J Sound Vib 2014;333(10):2840–62. https://doi.org/10.1016/j.jsv.2013.12.029.
[17] Gerist S, Maheri MR. Multi-stage approach for structural damage detection problem using basis pursuit and particle swarm optimization. J Sound Vib 2016;384:210–26. https://doi.org/10.1016/j.jsv.2016.08.024.
[18] Zhang G-M, Harvey DM. Contemporary ultrasonic signal processing approaches for nondestructive evaluation of multilayered structures. Nondestructive Testing and Evaluation. 2012;27(1):1–27. https://doi.org/10.1080/10589759.2011.577428.
[19] Ghose B, Balasubramaniam K, Krishnamurthy CV, Rao AS. Two dimensional FEM simulation of ultrasonic wave propagation in isotropic Solid Media using COMSOL. In COMSOL Conference 2010.
[20] Ghose B, Balasubramaniam K, Krishnamurthy CV, Rao AS. COMSOL based 2D FEM model for ultrasonic guided wave propagation in symmetrically delaminated unidirectional multilayered composite structures. Proceedings of the National Seminar and Exhibition on Nondestructive Evaluation, 2011.
[21] Wan X, Xu G, Zhang Q, Tse PW, Tan H. A quantitative method for evaluating numerical simulation accuracy of time-transient Lamb wave propagation with its applications to selecting appropriate element size and time step. Ultrasonics 2016;64:25–42. https://doi.org/10.1016/j.ultras.2015.07.007.